Present and Future of Modeling Global Environmental Change: Toward Integrated Modeling, Eds., T. Matsuno and H. Kida, pp. 89–99.

Tropospheric Chemical Transport Modeling over East Asia

Itsushi UNO[1,2]

[1]*Research Institute for Applied Mechanics/Kyushu University, Kasuga Park 6-1, Kasuga 816-8580, Japan*
[2]*Frontier Research System for Global Change, Tokyo 105-6791, Japan*

INTRODUCTION

Fast growing East Asian countries with their rapid increase in population and economy and, consequently, with their augmented energy consumption and production, show a dramatic increase in the emissions of air pollutants like sulfur and nitrogen oxides and particulates. As a consequence, acid deposition and long range transboundary air pollution are becoming one of the major concerns of the Environmental Protection Agencies in each country which have recently started to expand their monitoring activities.

Oceans such as the East China Sea, the Japan Sea between mainland China and Japan, as well as the Pacific Ocean cover a huge fraction of the region, and the interaction between the Pacific maritime air masses and continental air masses strongly affect the meteorology and climatology of East Asia. In particular, as a result of this interaction, storm tracks and orographic precipitation during the winter, the synoptic scale persistent precipitation belt related to the summer monsoon, and the passage of fast moving typhoons represent some of the climate features characteristic of this region (Emori *et al*., 2000). Therefore, knowledge of both the pollutant concentrations and meteorological parameters over these oceans is critically necessary to understand the long-range transport and transformation processes. However, there are very few observation points over these oceans, therefore, remote sensing observation (i.e., satellite) and/or simulations with a regional meteorological model become important tools to evaluate the spatial distribution of clouds and precipitation in this area.

To overcome these difficulties, an on-line regional scale chemical transport model fully coupled with CSU-RAMS (Regional Atmospheric Modeling System, Pielke *et al*., 1992) was developed to study regional transboundary air pollution. In particular, the coupled model can be adopted to simulate the regional meteorological climate and chemical composition climate over the Asian and West Pacific regions.

This study shows the role of meteorological and climatological conditions in the transboundary air pollution transport in East Asia and indicates the climatological changes in the chemical composition concentration and deposition by season.

NUMERICAL MODELS: RAMS AND ON-LINE TRANSPORT MODEL

The mesoscale model

The parallel version of the Regional Atmospheric Modeling System (RAMS version 4.28) has been used to simulate the regional scale 3-D meteorological fields including boundary layer turbulence, cloud and precipitation. In addition, an on-line tracer model fully coupled with RAMS was developed to study the long range sulfur transport and deposition. The Isentropic Analysis package (RAMS/ISAN) built into RAMS was used to model field initialization and four-dimensional data assimilation (FDDA) based on the ECMWF 2.5 degree global analysis data. FDDA involves the integration of effective time-dependent observational data into a predictive model. This can be done during a model run as in the Newtonian relaxation (nudging) scheme based on the assimilation of time-dependent lateral boundary conditions provided by the ECMWF global data.

The on-line long-range transport and deposition model

Sulfur transport and deposition is simulated using RAMS and an on-line long-range transport model. The chemical reaction and deposition processes are included to examine the transport and deposition from East Asian mainland towards Japan and the Pacific Ocean. The tracer model is fully coupled with RAMS, and this is a unique approach because the regional meteorological conditions, which play a significant role in the wet deposition and vertical diffusion of tracers, are continuously updated within the tracer model at the same time intervals, and the transport and deposition processes can be directly handled using real time meteorological parameters from the mesoscale model. The chemical tracer model can simulate the SO_2, sulfate and yellow sand transport and

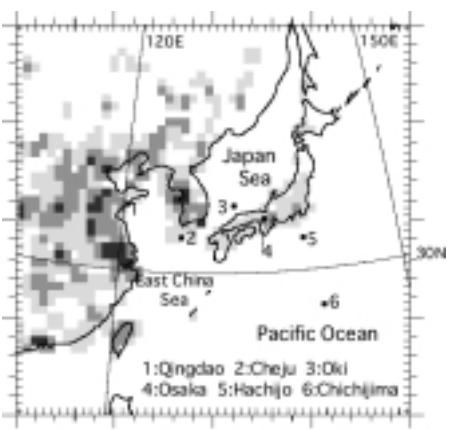

Fig. 1. Model domain and site locations analyzed in the paper (#1–#6). Tone color darkness (3 levels) represents the SO_2 emission relative intensity of 1, 5, 20 strength.

transformation processes, and the aerosol concentration can be fedback to the atmospheric radiation budget of RAMS (feedback is not included in this study).

A crucial point in the transboundary air pollution and the wet and dry deposition modeling are the removal rates and chemical conversion rates adopted in the model. Particular attention must be paid to the SO_2 conversion rates to sulfate. Despite these complex chemical conversion mechanisms, at present stage, the on-line transport model includes the linear chemical reaction from SO_2 to SO_4^{2-} in the gas phase by $SO_2 + OH \rightarrow SO_4^{2-}$. In the aquaous phase, the transport model includes two major reactions of $S(IV) + O_3(aq) \rightarrow SO_4^{2-}$ and $S(IV) + H_2O_2(aq) \rightarrow SO_4^{2-} + H_2O$. The main gas and liquid phase chemical reactions between SO_2 and SO_4^{2-}, and their respective rate coefficients used in the on-line tracer model in their simplified form are taken from Pham *et al*. (1995) and Takemura *et al*. (2000). Seasonal variations in the O_3 and H_2O_2 concentrations are assured based on the results reported by Takemura *et al*. (2000). It also includes dry deposition as well as wet scavenging of these species based on the precipitation rate.

Numerical simulations setting

The simulation domain adopted is centered at 35N, 130E, and it covers a large part of East Asia, including all of Japan, North and South Korea, most of China, and parts of Russia and Mongolia (Fig. 1). The horizontal grid consists of 50 by 50 grid points, with a resolution of 80 km. In the vertical direction, the domain is divided into 23 layers (top level is 20 km) and a terrain following coordinate has been used. The mesoscale model has been initialized using ECMWF data at a 2.5 degree resolution, with the sea surface temperature (SST) from the NCEP database (1 degree resolution). A strong nudging is prescribed every 12 hours for the outer 5 lateral grid cells of the domain. Note that even though the ECMWF data has a resolution lower than the model, however, it is still good enough to provide appropriate external forcing (i.e., the large-scale meteorological conditions) to the simulation region. To simulate the transport and deposition of anthropogenic pollutants in East Asia, the SO_2 emission dataset at 1×1 degree resolution is used (Akimoto and Narita, 1994). As shown in Fig. 1, a large SO_2 emission intensity is concentrated over the east coast of China (approximately 20 million ton/year based on the year 1987 statistics).

The actual integration has been performed on a Pentium III Linux Cluster system of 16 processors, which provided the opportunity to test the entirely parallelized version of the code, including the on-line tracer module under several conditions. The use of a cluster of Pentium III processors not only significantly reduces the CPU time of the simulations, but it also abates the costs of the simulations to a minimal fraction compared to other parallel clusters.

The numerical integration covered a 12 month periods: from April 01, 1994 0 UTC until April 1, 1995 0 UTC, and results from the simulations have been compared to observations from several monitoring stations (location is shown Fig. 1). The CPU elapsed time for the 12 month simulation with a 90-sec time step is 40.8 hours.

REGIONAL CLIMATE AND CONCENTRATION VARIATIONS

Previous studies pointed out that the wind pattern variations associated with the synoptic scale pressure system changes have a key role in the transboundary air pollution transport (Uno *et al*., 1997) in East Asia. The dramatic variation in the topography and land type of this region, and the altering of the large industrial/urban centers and agricultural/rural areas, together with the interactions between the continental and marine air masses strongly influence the large scale flow patterns, and play a prominent role in determining the effects of pollutant production and transport in the region. In fact, the East China Sea, the Japan sea and the Pacific Ocean cover a huge fraction of east Asia, therefore, the knowledge of pollutant concentrations and meteorological parameters over these water masses are critically necessary to understand the long-range transport and transformation processes.

The important climate features of the region, schematically represented in Fig. 2, show, for each season, a typical pattern depending on the relative strength of the Pacific high and continental high pressure systems.

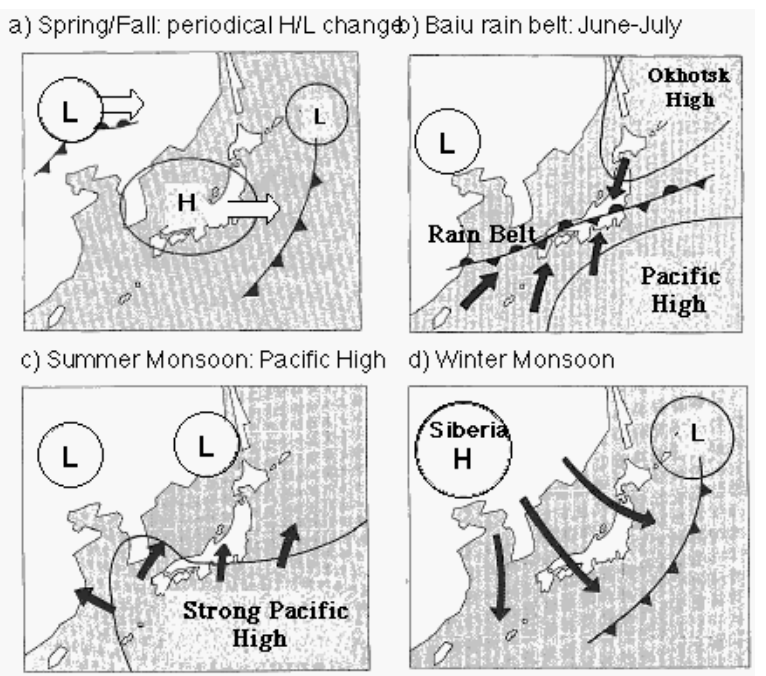

Fig. 2. Important regional climate/weather pattern over East Asia. (a) Spring/Fall travelling high/low pattern, (b) Baiu rain season pattern, (c) summer monsoon pattern, (d) winter monsoon pattern.

A large scale traveling high/low pressure system, moving slowly eastward is characteristic of the spring/fall weather (Fig. 2(a)). The Baiu rainy season, characterized by the presence of a rain belt with heavy precipitation, strongly affects the wet deposition in the region during late spring–early summer (Fig. 2(b)). The distribution of this rainfall amount in the belt is non-uniform and the location of the associated rainbelt zone oscillates in the south-north direction due to the relative strength of the Pacific and continental high pressure systems. The air mass under the Pacific high pressure system is relatively clean while the air mass under the continental high is usually polluted due to the existence of the intense emission area.

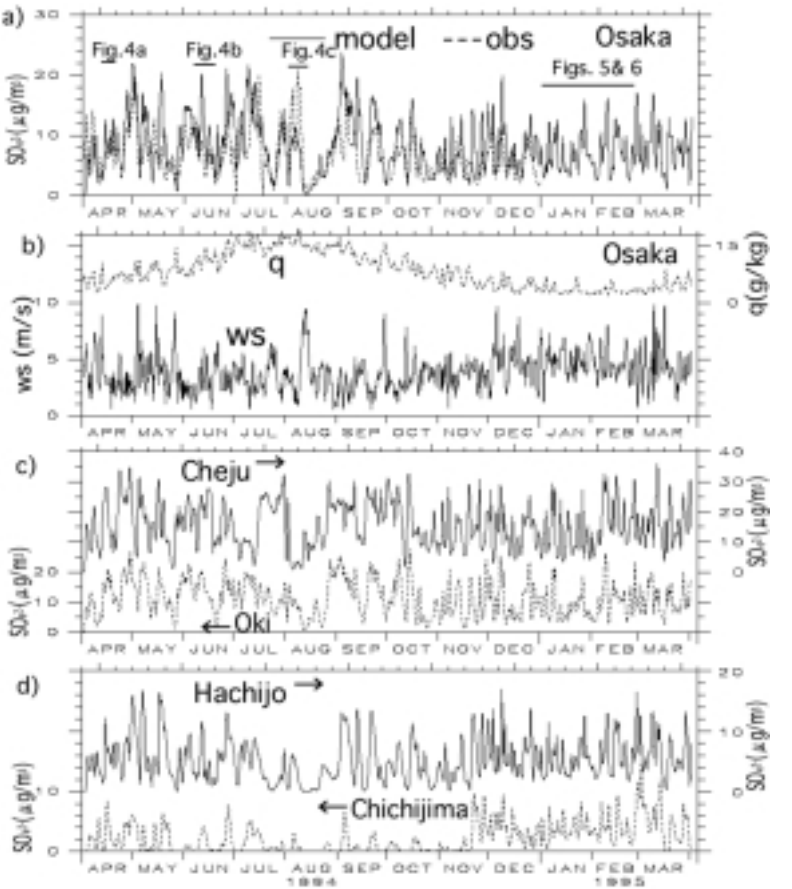

Fig. 3. (a) SO_4^{2-} concentration variation at Osaka (location #4 in Fig. 1). Models 12-hours averaged concentration (straight line) and daily averaged observation (dot line), (b) specific humidity and surface wind speed at Osaka, (c) SO_4^{2-} concentration variation at Cheju (Korea) and Oki, (d) SO_4^{2-} concentration variation at Hachijo and Chichijima.

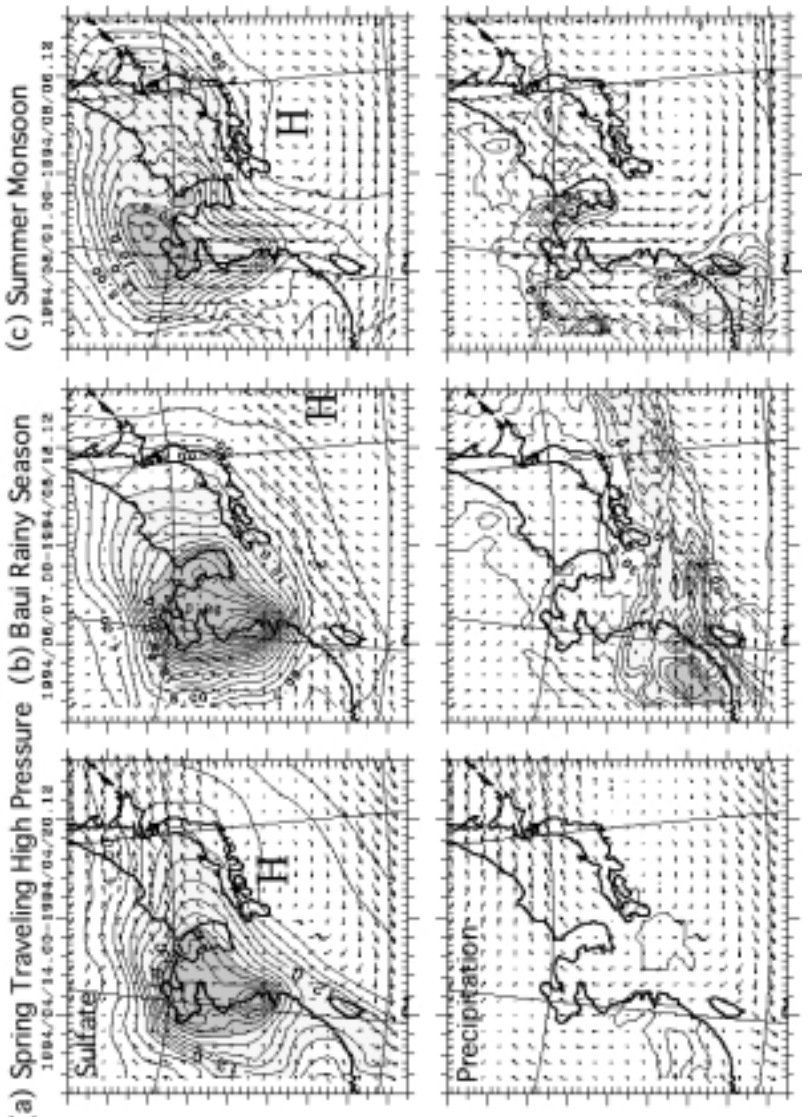

Fig. 4. Upper raw is averaged surface SO_4^{2-} concentration ($\mu g/m^3$), wind fields and lower raw shows accumulated precipitation (mm) during (a) April 14–April 20, (b) June 7–June 18, (c) August 1–August 6, 1994.

When the Pacific high pressure system becomes stronger, the rain-belt then disappears and the Japanese area is covered by a Pacific high, which characterizes the typical summer monsoon (Fig. 2(c)). Under this condition, relatively the clean and hot/moist air dominates the East Asia domain.

Finally typical winter monsoon is shown in Fig. 2(d). From the middle of November to early March, strong pressure gradients between Siberia (Continental) High and Okhotsk Low exist on average, which follows the strong winter monsoon in the region. This typical winter monsoon usually lasts a few days, and after this, a low pressure system develops and moves from the China continent to the eastside of Japan as the transition of the weather change. Such a transition pattern is usually observed 1–2 times per week.

These seasonal regional climate changes play a significant change in the regional air quality. Twelve month time series of some key meteorological parameters such as wind speed, water vapor content at several sites in the region have been analyzed in order to show the different climatological seasonal patterns (Fig. 3). The precipitation pattern prediction from RAMS plays an important role and the performance of the precipitation fields has been analyzed in detail in previous studies (Emori *et al.*, 2000) and show a good agreement with the observation data, which will not be discussed here.

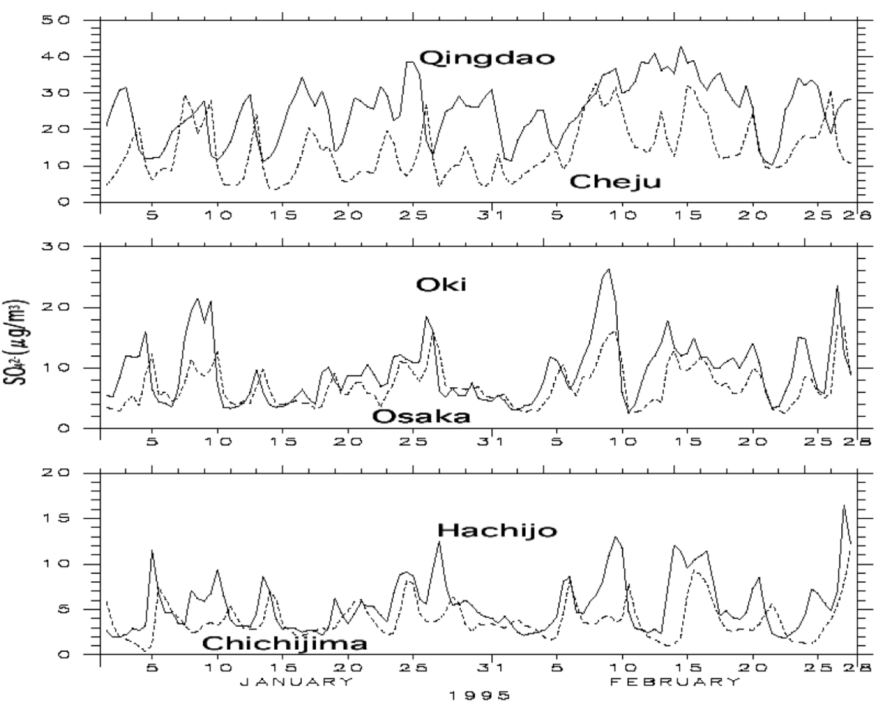

Fig. 5. Time variation of SO_4^{2-} concentration during winter monsoon in January–February 1995 at Qingdao (China), Cheju (Korea), Oki, Osaka, Hachijo and Chichijima.

Figure 3(a) shows the SO_4^{2-} concentration variation at Osaka (location #4 in Fig. 1). The modeled 12-hour averaged concentration (straight line) and daily averaged observation (dot line) are shown in the figure. Figure 3(b) shows the specific humidity and surface wind speed at Osaka. Figures 3(c) and (d) show the SO_4^{2-} concentration variation at Cheju, Oki, Hachijo and Chichijima (Locations are shown in Fig. 1). The observed sulfate concentration at Osaka compared with the model results shows a good agreement, and the intermittency during the winter season and the periodicity typical of the spring/fall rainy seasons, when the change of high/low pressure systems characterize the meteorology of the region, is nicely reproduced by the numerical model. One of the surprising facts is the time variation among these 5 stations in winter shows a very similar spiky pattern that will be discussed later.

Some specific periods have been analyzed in order to have a better understanding of the seasonal differences in the typical regional climatology and the variations in the sulfate concentration (Figs. 4–6).

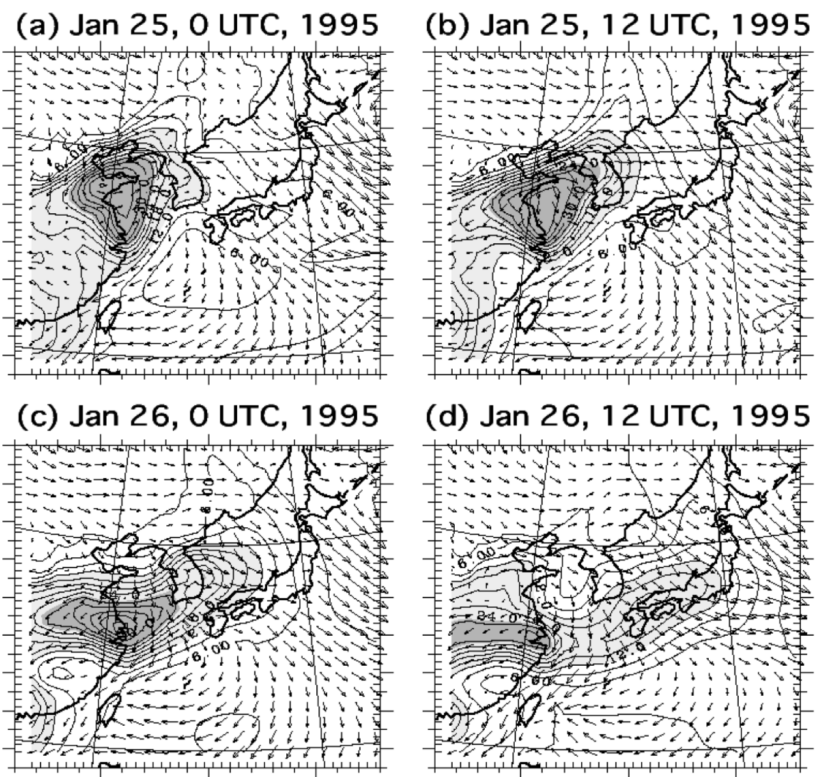

Fig. 6. Snapshot of SO_4^{2-} outbreak occurred from January 25 to January 26, 1995. Contour interval is every 3 ($\mu g/m^3$)

At first, for each season, selected typical weather patterns (Figs. 2(a), (b) and (c) patterns) have been chosen with their associated sulfate concentrations and accumulated precipitation amount (Fig. 4). The averaged flow field, SO_4^{2-} concentration and precipitation from April 14 to April 20 are shown in Fig. 4(a), which represents the typical spring time travelling high pressure pattern. Almost no precipitation was observed and the clockwise outflow at the northern edge of high pressure system transports the pollutants toward the northern part of Japan. Figure 4(b) shows the averaged field from June 7 to June 18, which represents the rainy season shown in Fig. 2(b). It clearly shows that the high concentration is trapped north of the rain belt. Figure 4(c) shows the typical summer monsoon pattern already shown in Fig. 2(c). A strong outflow from the Pacific high and precipitation occur in the northern part of China and Korea, and pollutants are transported to these precipitation zones.

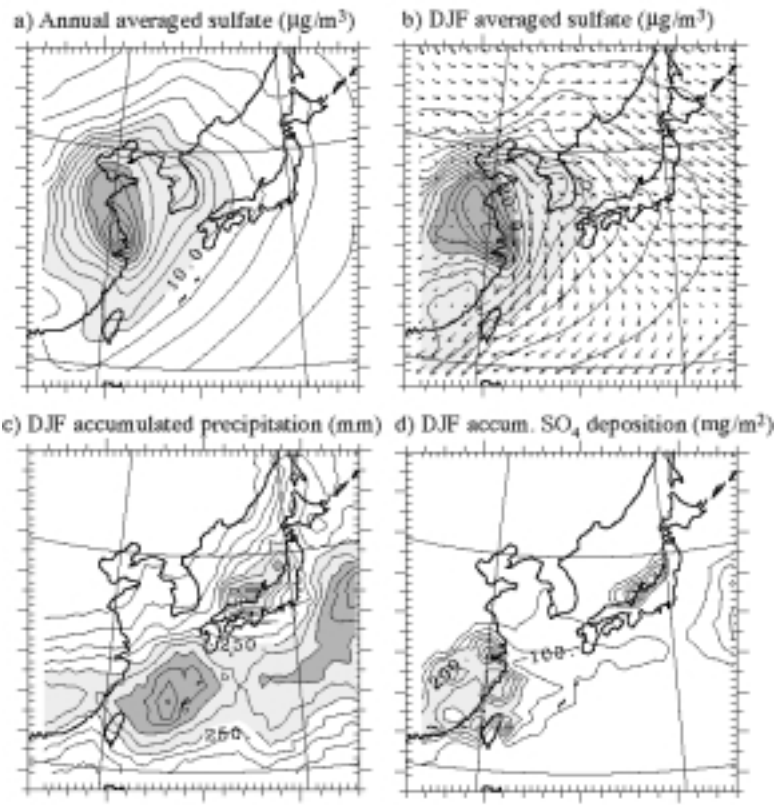

Fig. 7. (a) Surface level annual averaged SO_4^{2-} concentration ($\mu g/m^3$), (b) DJF (Dec.-Jan.-Feb.) averaged SO_4^{2-} concentration ($\mu g/m^3$) and wind fields, (c) DJF accumulated model precipitation (mm) and (d) DJF accumulated ($\mu g/m^3$) wet deposition field (mg/m^2).

Secondly, some analysis details in winter monsoon are shown in Fig. 5. It shows the time variation of the SO_4^{2-} concentration during winter monsoon in January–February 1995 at the 6 locations shown in Fig. 1. Figure 6 shows a snapshot of the sulfate concentration outbreak that occurred from January 25 to January 26, 1995. The winter season is characterized by the intermittent outbreak of cold/dry air masses carrying air pollution from mainland Asia towards the Pacific Ocean and over Japan. Such an intermittence is clearly shown in the time series of SO_4^{2-} concentration. As shown in the snapshot at Fig. 6, low pressure systems, moving southeasterly from the China mainland to the eastside of Japan bring pollution as far as Chichijima, and a clear footprint of the motion of such cyclonic systems is given by the SO_4^{2-} concentration time series from several sites in the domain. The concentration peak time within the 6 sites clearly shows a time lag (it takes about 2–3 days from Qingdao to Chichijima). This time delay can be explained by the "ice-cream cone cup" like polluted air mass outbreak shown in Fig. 6.

ANNUAL SULFATE CONCENTRATION AND DEPOSITION

The chemical climatic representation of the sulfate field is important for understanding the several environmental impacts for acidification. Figure 7 shows the surface level annual averaged sulfate concentration (Fig. 7(a)), DJF (Dec.–Jan.–Feb.) averaged sulfate concentration and wind field (Fig. 7(b)), model precipitation (Fig. 7(c)) and wet deposition field (Fig. 7(d)). The annual averaged sulfate concentration fields over the China mainland are strongly affected by the horizontal distribution of the SO_2 emission intensity shown in Fig. 1. The contour lines of the annual averaged sulfate field show a distribution parallel to the ideal line connecting the Taiwan and Japan Islands in the SW-NE direction, with a gradient more gentle than over the mainland. The sulfate concentration differences on the Japan mainland is within a factor of 2. During the winter (DJF), the southern part of China and Taiwan show concentration values higher than the annual averaged value, and the continental outflow pattern shown in Fig. 7(b) is responsible for these differences. In addition, the Japan sea side, the southern part of the East China sea and the north Pacific ocean are affected by large precipitation amounts. In particular, the continental outflow passing over the warm Japan sea is the main reason of the large precipitation on the Japan seaside. As shown in Fig. 7(b), the sulfate concentration level on the Japan seaside is lower than on the mainland, however, the wet deposition amount in this region is higher than expected, because the wet scavenging is due to the combination of sulfate and the precipitation rate.

The calculated wet deposition amount is strongly affected by the local precipitation rate (including in-cloud scavenging rate) and the sulfate concentration field. The model predicted an annual SO_4 wet deposition over the Japanese area ranges between 100–500 SO_4-mg/m^2, which is still lower than the observed results. A further modeling study is necessary to reproduce the wet deposition distribution over east Asia, especially the aquaous phase SO_2 oxidation reaction model and the in-cloud scavenging model are critically important to improve the current modeling performance.

CONCLUDING REMARKS

The present paper shows the role of meteorology and climatology in the transboundary air pollution transport in East Asia, and indicates the climatological changes in the chemical composition concentration and deposition by season. The numerical experiments using the Pentium III–Linux 16 CPU cluster system successfully simulated the regional climate over a 12-month time period. The surface concentration, and dry/wet deposition amount of sulfate, modeled using a chemical model fully coupled with the mesoscale model, show patterns consistent with the climatology of the region both on an annual and seasonal scale, which explain the important meteorological condition for transboundary air pollutants transport in East Asia, and indicates the dramatic changes in the chemical composition concentration by season. In addition, the coupled model is able to correctly simulate the specific episodes. However, the absolute values of the sulfate concentration and accumulated deposition, although comparable with observations, are not completely satisfactory and the chemical model requires more improvements. In particular, the wet scavenging and SO_2 oxidation reaction processes, not fully implemented in the present stage on-line tracer model, due to the complexity of those processes, must be more accurately parameterized.

Acknowledgements—This work is supported by Core Research for Evolution Science & Technology (CREST; PI Prof. Mitsuo Uematsu of Tokyo University) and Research and Development Applying Advanced Computational Science and Technology of Japan Science and Technology Corporation (ACT-JST). The authors are grateful to the Prof. Akira Mizohata of Osaka Prefectural University for providing the sulfate observational data.

REFERENCES

Akimoto, H. and H. Narita, 1994: Distribution of SO_2, NO_x and CO_2 emissions from fuel combustion and industrial activities in Asia with 1×1 resolution. *Atmos. Environ.*, **28**, 213–225.

Emori, S., T. Nozawa, A. Numaguti and I. Uno, 2000: A regional climate change projection over East Asia. *Proceedings of AMS 11th Symposium on Global Change Studies*, 15–18, January, Long Beach, U.S.

Pham, M., J.-F. Muller, G. P. Brasseur, C. Granier and G. Megie, 1995: A three-dimensional study of the tropospheric sulfur cycle. *J. Geophys. Res.*, **100**, D12, 26061–26092.

Pielke, R. A., W. R. Cotton, R. L. Walko, C. J. Tremback, W. A. Lyons, L. D. Grasso, M. E. Nicholls, M. D. Moran, D. A. Wesley, T. J. Lee and J. H. Copeland, 1992: A comprehensive meteorological modeling system—RAMS. *Meteorol. Atmos. Phys.*, **49**, 69–91.

Takemura, T., H. Okamoto, Y. Maruyama, A. Numaguti, A. Higurashi and T. Nakajima, 2000: Global three-dimensional simulation of aerosol optical thickness distribution of various origins. *J. Geophys. Res.*, **105**, 17853–17873.

Uno, I., T. Ohara and K. Murano, 1997: Simulated acidic aerosol long-range transport and deposition over east Asia—role of synoptic scale weather systems. *22nd NATO/CCMS International Technical Meeting on Air Pollution Modeling and Its Application*, 119–126, June, France.

I. Uno (e-mail: iuno@riam.kyushu-u.ac.jp)